Structural Engineering and Mechanics, Vol. 32, No. 5 (2009) 587-608 587
DOI: http://dx.doi.org/10.12989/sem.2009.32.5.587

Development of analytical modeling for an energy-dissipating cladding panel

H. Maneetes† and A. M. Memari‡

Department of Architectural Engineering, The Pennsylvania State University, 104 Engineering Unit A, University Park, PA, 16802, U.S.A.

(Received July 15, 2008, Accepted June 11, 2009)

Abstract. Modern earthquake-resistant design aims to isolate architectural precast concrete panels from the structural system so as to reduce the interaction with the supporting structure and hence minimize damage. The present study seeks to maximize the cladding-structure interaction by developing an energy-dissipating cladding system (EDCS) that is capable of functioning both as a structural brace, as well as a source of energy dissipation. The EDCS is designed to provide added stiffness and damping to buildings with steel moment resisting frames with the goal of favorably modifying the building response to earthquake-induced forces without demanding any inelastic action and ductility from the basic lateral force resisting system. Because many modern building facades typically have continuous and large openings on top of the precast cladding panels at each floor level for window system, the present study focuses on spandrel type precast concrete cladding panel. The preliminary design of the EDCS was based on existing guidelines and research data on architectural precast concrete cladding and supplemental energy dissipation devices. For the component-level study, the preliminary design was validated and further refined based on the results of nonlinear finite element analyses. The stiffness and strength characteristics of the EDCS were established from a series of nonlinear finite element analyses and are discussed in detail in this paper.

Keywords: precast concrete; spandrel cladding panels; earthquake energy dissipation; finite element analysis; analytical modeling.

1. Introduction

Architectural precast concrete cladding systems are considered as non-load bearing wall systems and are designed primarily to transfer their self-weight and out-of-plane (wind and earthquake) lateral loads to the supporting building structure. The contribution of the cladding system to the lateral stiffness of the building is often ignored in the structural design. Studies (Ellis 1980, Goodno and Will 1978, Wiss and Curth 1970) have shown that these architectural components can contribute significantly to the lateral stiffness of the structure and that the panels can be subjected to significant in-plane forces. Other researchers (El-Gazairly and Goodno 1989, Meyyappa *et al.* 1981, Uchida *et al.* 1973) have shown that the precast cladding panels can have significant effect on the dynamic properties of the building.

† Former Graduate Student
‡ Associate Professor, Corresponding author, E-mail: amm7@psu.edu

Modern earthquake-resistant design requires that these cladding panels be isolated from the lateral load resisting system. This is to prevent the panel from participating in the building response and hence minimizing the type of cladding damages (Arnold *et al*. 1987) seen in the 1978 Miyagiken-Oki, 1987 Whittier Narrows and the 1995 Hyogoken-Nambu earthquakes (McMullin 2000). Flexible connections or connections that allow relative movements at the attachment points as suggested by PCI (1989), are all conceived to minimize the cladding-structure interaction. On the other hand, post-earthquake observations have revealed that these qualified cladding connection details would still induce some form of interaction effect between cladding and structural system (Pinelli *et al*. 1993) and could restrain the racking deformation of the structural frame, and significantly stiffen it against any lateral loading (Gaiotti and Smith 1992).

Rather than emphasizing the need to minimize cladding-structure interaction, some researchers have made efforts in the opposite direction that seeks ways to maximize the benefits of cladding-structure interaction while attempting to minimize the damaging effect on the cladding panels. For example, Goodno *et al.* (1992) exploited this cladding-structure interaction through the development of an advanced energy dissipating mechanism in the cladding connections.

However, existing studies on the special energy dissipating cladding system were confined to story high or floor-to-floor type cladding panels that span from one floor to an adjacent floor. As shown in Fig. 1, Modern building facades typically have continuous and large openings on top of the spandrel beams or precast cladding panels at each story for the installation of windows or ventilation requirement as in for open parking structures. Existing concepts developed for energy-

Fig. 1 Spandrel cladding panels used as the building facade

dissipating cladding panels are not necessarily applicable to conventional spandrel type panels that are supported on and attached only to one floor and not directly affected by interstory drift.

This paper is based on the results of a research program that was aimed at enhancing the performance of the building seismic response by using the implicit advantage of the building enclosure integrated in the lateral load resisting system of the building. The primary objective of the research was to develop an added energy-dissipating system, which can be applicable specifically to spandrel type precast concrete cladding panels, although the concept could also be applied to floor-to-floor high panels. This spandrel type Energy-Dissipating Cladding System (EDCS) would be able to function as a structural brace while providing some form of controlled energy dissipation. The main design criterion for this system is to ensure that no damage will be incurred on the structural system and the cladding panel and its connections as a result of the cladding-structure interaction. More importantly, the present design seeks to implement the EDCS as a form of a distributed structural bracing system. In the following sections, after discussion of the conceptual design of EDCS, finite element modeling of the precast concrete panel and simplified analytical modeling of stiffness properties are presented.

2. Conceptual design

Partial height spandrel type bracing is a departure from conventional full-height bracing systems (e.g., concentrically-braced, eccentrically-braced). Preliminary analytical studies (Maneetes 2007) have shown that such bracing system on a moment resisting frame can be an effective Lateral Force-Resisting System (LFRS) by virtue of its numbers and its location in the building envelope. The preliminary studies have also shown that friction damper would be an appropriate damper type for the spandrel type bracing system to provide additional form of energy dissipation.

The design of the EDCS followed as close as possible that of conventional precast concrete cladding system so as to improve constructability and to minimize production cost. A typical spandrel type cladding panel has two bearing connections for supporting its own weight and at least two flexible tie-back connections to transfer out-of-plane loads while accommodating the in-plane movement. The conventional earthquake-resistant design of precast concrete panel suggested by PCI (1989) is directed at isolating the cladding panel from the structural frame thereby minimizing damage resulted from cladding-structure interaction. Spandrel cladding panel with tie-back connections attached to the same floor beam as bearing connections is not affected by story drift since the entire set of connections move together with the floor beam. For spandrel panel with tie-back connections attached to the columns, the flexible tie-back connections provide the necessary isolation to prevent the structure's seismic lateral force from transmitting to the panel. In effect, the panel can be designed as a non-structural element such that it would not be necessary to consider the panel interaction in the dynamic response of the structure; however, it is noted that the heavy panels have a contribution to the effective seismic weight of the building). Other researchers (Craig *et al.* 1992, Pinelli *et al.* 1993, Goodno and Craig 1998) have designed advanced type of connections that behave as hysteretic energy dissipation mechanisms.

In order for the EDCS to function both as a structural brace and a source of energy dissipation, the following factors were considered.

1. The EDCS must be capable of transferring the developed in-plane force in an elastic manner without deterioration of strength or stiffness under cyclic loading.

2. Based on separate analytical studies (Maneetes 2007), friction-based energy dissipating system was found be the most appropriate for the EDCS. The device must be incorporated into the bracing system of the EDCS.
3. At least one of the support connections of the EDCS must be restrained in both vertical and lateral directions to transfer the load from the supporting beam to the precast concrete panel. The other bearing connections must be capable of resisting uplift due to the action of the lateral load while permitting volume changes in the panel.
4. While tie-back connections can still be used to transfer out-of-plane loads, some form of connection must be provided that could transfer the high in-plane force from the column to the EDCS.

Fig. 2 shows the proposed concept of the EDCS that is designed to engage the cladding-structure interaction. The key EDCS components are shown in Fig. 3. The friction damper is installed on the concrete panel surface and is designed as part of the connection between column and the top of the cladding panel. The friction damper is designed to slip horizontally, thus maximizing the drift effect. The precast concrete panel would function as a rigid brace during low intensity earthquake motions. Under moderate or high intensity seismic motions, the force developed in the cladding panel would

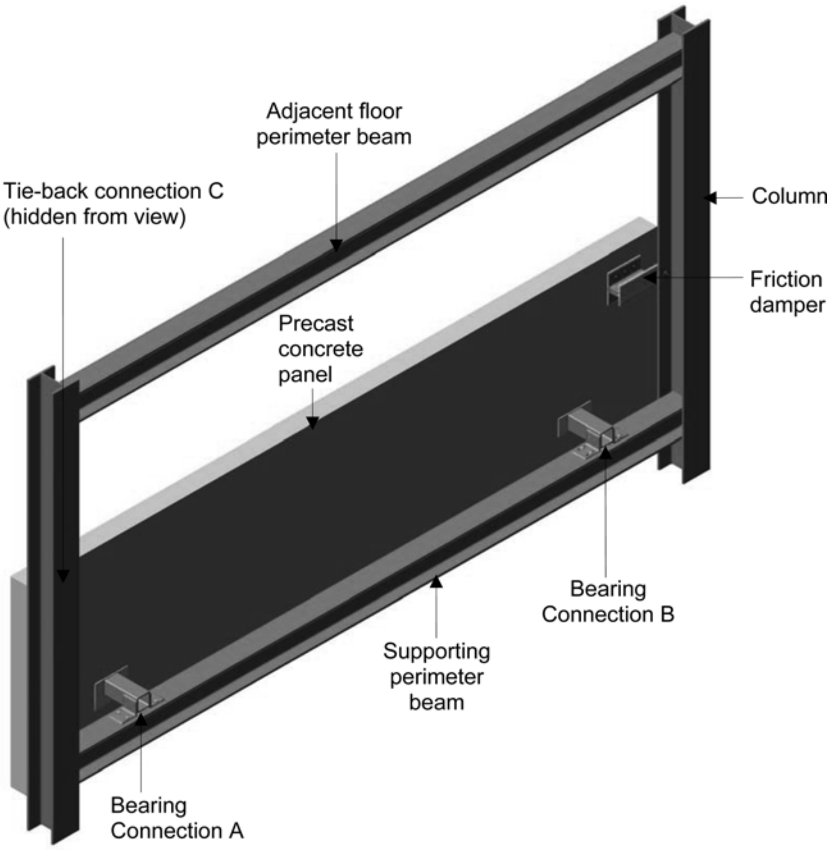

Fig. 2 Proposed EDCS concept

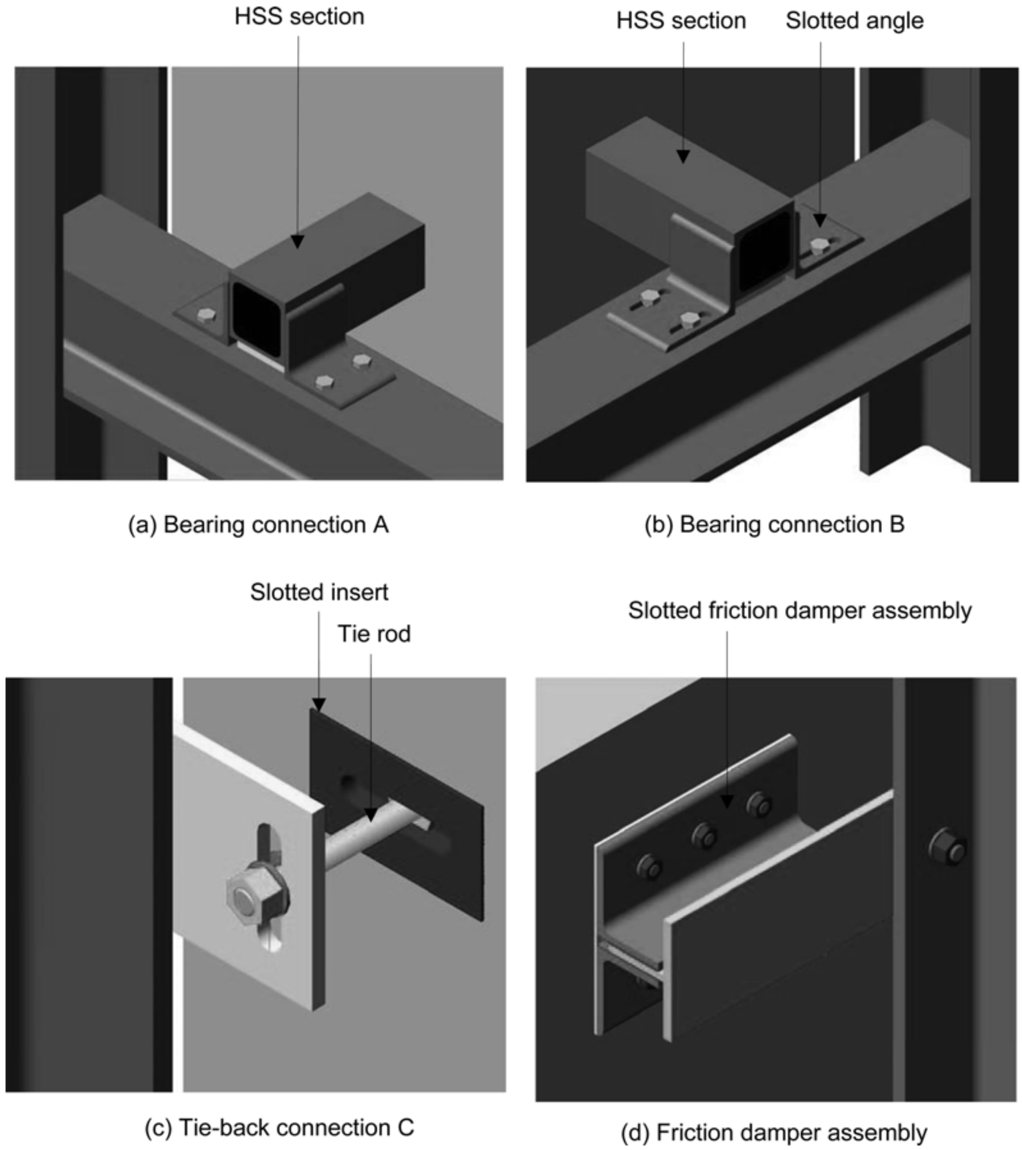

Fig. 3 Proposed EDCS components

reach the slip load of the friction damper, causing it to slip and dissipate part of the building input energy. In this regard, the friction damper has an important function of limiting the maximum load that can be transferred to the concrete panel.

One of the support bearing connections is bolted (and welded) to supporting beam/floor while the other bearing connection is restrained from uplift but is designed (through the use of slotted connection) to translate laterally to accommodate volume changes in the panel. The friction damper is incorporated as part of the connection between the column and the cladding panel. The friction damper (Pall *et al.* 1980) serves two important functions: a source of energy dissipation and a “safety fuse” that effectively limits the amount of in-plane force that would be transferred into the concrete panel. The friction damper type designed is adopted from the Slotted Bolted Connection (SBC) design proposed by Grigorian *et al*. (1993). Details of the friction damper designed are discussed in Maneetes (2007). Because the proposed design relied on the ability of the precast concrete panel to carry the high in-plane loads, it had to be designed accordingly. It should be pointed out that the proposed EDCS design was conceived for the use of the connection details (e.g., tie-back, bearing connections) typical of conventional precast cladding system. This choice was intended to minimize production and installation cost.

3. Finite element modeling

Precast concrete panels, especially architectural precast cladding panels, are not designed for significant structural forces. This may explain why there seems to be inadequate literature on the Finite Element Analysis (FEA) of precast concrete panels. The finite element model of the panel is often idealized as uncracked and infinitely stiff (Petkovski and Waldron 1995, Goodno and Craig 1998). The panel connections to the structural frame appear to be the focus of most research interest since the connections could turn out to be the weakest link in the event of a catastrophic failure. For the present research, the precast concrete panel, as part of the EDCS, is designed to participate in the building LFRS. Therefore, it is important to better understand the strength and stiffness characteristics of the concrete panels subjected to significant in-plane loading.

The spandrel panel studied is shown in the Fig. 4. The panel is 2.13 m (7 ft) high (based on one-third height configuration). The panel height takes into account the depth of supporting beam, concrete floor slab, raised-floor requirement (in typical office), finishes, etc. and also height to openings (i.e., window). The panel is 7.32 m (24 ft) long and 203.2 mm (8 in.) thick. This length corresponds to that of a typical bay. According to PCI Design Handbook (PCI 2004), structural welded wire reinforcement (WWR) is commonly used to satisfy the serviceability requirements (i.e., shrinkage and cracking control) due to ease of placement. Supplementary reinforcements were also added to better confine the concrete at the highly stressed connection anchoring points, hence preventing the development of localized cracking. To transfer the in-plane applied force through the panel, different schemes of placing the extra reinforcing bars were investigated.

HSS6x6x1/2 was used for the bearing connections while 25.4 mm (1 in.) diameter rod was specified for the tie-back. Two configurations to anchor the bearing connections to the concrete panel were proposed. The Headed Concrete Anchors (HCA) used in the EDCS comprised of a 508

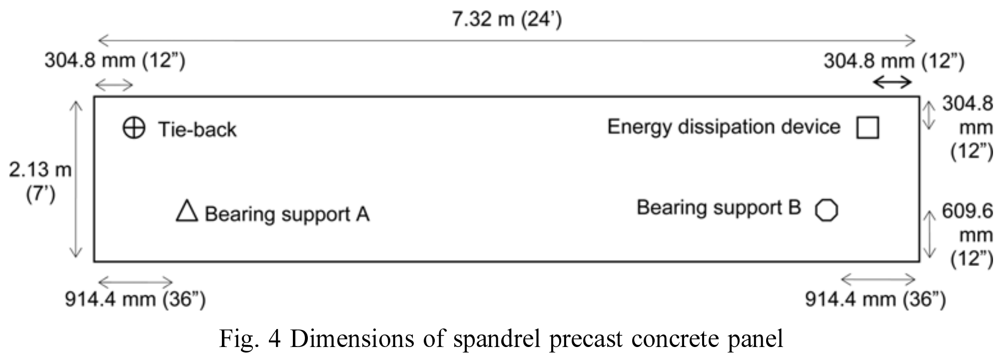

Fig. 4 Dimensions of spandrel precast concrete panel

mm (20 in.) long by 304.8 mm (12 in.) wide by 50.8 mm (2 in.) thick anchorage plate with eight 22.2 mm (7/8 in.) diameter by 152.4 mm (6 in.) headed studs. Based on PCI design guidelines (PCI, 2004), the nominal design tensile and shear capacities of the HCA group were calculated as 282 kN (63.4 kips) and 94.3 kN (21.2 kips) for corner condition, respectively. Additional bars (with adequate development length) were attached to plates in two orthogonal directions to increase the shear capacity (in excess of 266.9 kN or 60 kips).

Several recent studies (Wolanski 2004, Fanning 2001, Idelsohn *et al.* 1998) have focused on a commercial FE package, ANSYS, for modeling reinforced concrete beams and prestressed beams. These studies have reported good correlations between the analytical results and experimental data. This is largely attributed to the availability of a rather sophisticated element, known as SOLID65, from ANSYS element library. This element was developed primarily to model the complex nonlinear behavior of brittle materials, especially plain concrete and reinforced concrete. In particular, the complex cracking phenomenon of concrete can be modeled with its built-in cracking models. The availability of this exclusive concrete element, together with good correlations reported by these studies, has made ANSYS (Version 9) a preferred FE software for modeling precast concrete cladding panels for the present research. The appropriateness of the modeling strategies described below for the reinforced concrete and HCA were verified by separate FEA studies.

A total of 6,003 SOLID65 elements were used for the concrete panel. The Hognestad stress-strain relationship with multi-linear kinematic hardening rule was used. The cracking model in the

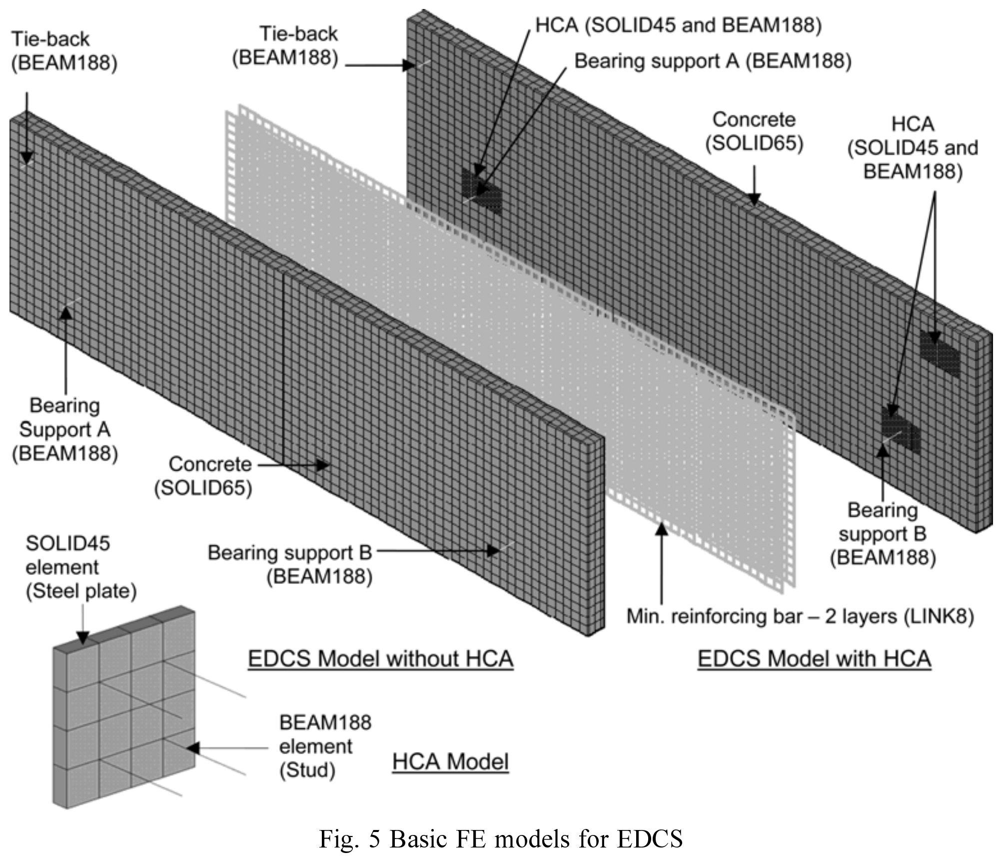

Fig. 5 Basic FE models for EDCS

SOLID65 element was employed. All relevant material properties for the concrete were specified for a concrete strength of 34.48 MPa (5,000 psi). The basic FE models for the concrete panel are shown in Fig. 5. Different amount and arrangement of additional reinforcing steel were investigated.

The HSS section (for the bearing supports) was modeled with BEAM188 elements. Where anchorage plate was used (e.g., for HCA), the BEAM188 elements were embedded into the SOLID45 (steel plate) elements. This was required to prevent unnecessary rotations at the plate-beam interface. It should be pointed out that the "stick" BEAM188 element has practically zero "foot-print" that could lead to unrealistically high stress concentration occurring in the adjacent SOLID45 plate elements leading to excessive flexure of the plate. In reality, the (welded) base of the actual HSS covered a finite area of the plate and this portion of the plate could be considered as infinitely stiff; any significant plate bending would occur outside this area. Thus, it would not be inaccurate to specify a high rigidity for the SOLID45 plate elements confined within this area.

The threaded-rod for the tie-back connection was modeled with BEAM188 element. It could have been defined with the simpler LINK8 spar element since its response was mainly uniaxial tension-compression. The LINK8 element was specified for all reinforcing bars in the concrete and placed in accordance to the layout specified for each analysis case (as discussed in the next section). A concrete cover of 25.4 mm (1 in.) was used.

The nonlinear behavior of the friction damper is generally well-understood and could be modeled using ANSYS COMBI165 spring-damper element. Adding the friction damper in the FE model would effectively limit the maximum load of the EDCS to the damper slip load. In this case, the EDCS components (i.e., concrete panel and connections) would merely respond elastically as designed. Although not critical, it would be more useful to obtain information about the inelastic response of these components, for example the onset of inelastic response. Thus, the friction damper was excluded from the FE model to achieve higher loads and inelastic component response.

A concentrated load and moment were simultaneously concentrically applied to the surface of the anchorage plate. The moment accounted for the out-of-plane load eccentricity of 254 mm (10 in.) For the bearing supports, the free end of the BEAM188 element was specified as pinned or fixed for support A, depending on the analysis case, and roller (horizontal direction) condition for support B. The tie-back is capable of resisting out-of-plane force only.

A total of eight models corresponding to different reinforcing layout and connection details were analyzed. From the load-deformation plots (Fig. 6), the initial tangent stiffness, maximum load, the elastic-limit load (i.e., load at the onset of nonlinear response) for each case are summarized in Table 1. The numerical results showed that the extent of cracking at the connections controlled the maximum load at which each analysis could reach.

Model cp1 was developed to represent conventional architectural precast cladding panel. It was specified with minimum reinforcement with no additional steel reinforcing bars near the connections. The FEA for model cp1 terminated at a very low load (9.2 kips) due to extensive cracking around the loading point. Although this load may not necessarily the ultimate lateral load capacity of the panel, the stiffness of the panel was deteriorating rapidly beyond this load level. This was not desirable since the concrete panel was expected to behave essentially elastic up to about 177.9 kN (40 kips) (i.e., twice the designed slip load). The numerical crack pattern observed was consistent with a corner failure (Maneetes 2007). For model cp2, diagonal bars (or sections) were added to provide a direct load path directly between the pinned support with the aim of improving the lateral load carrying capacity. The analytical results show that the increase in lateral stiffness was insignificant. Based on the stress results in the diagonals, it was found that the

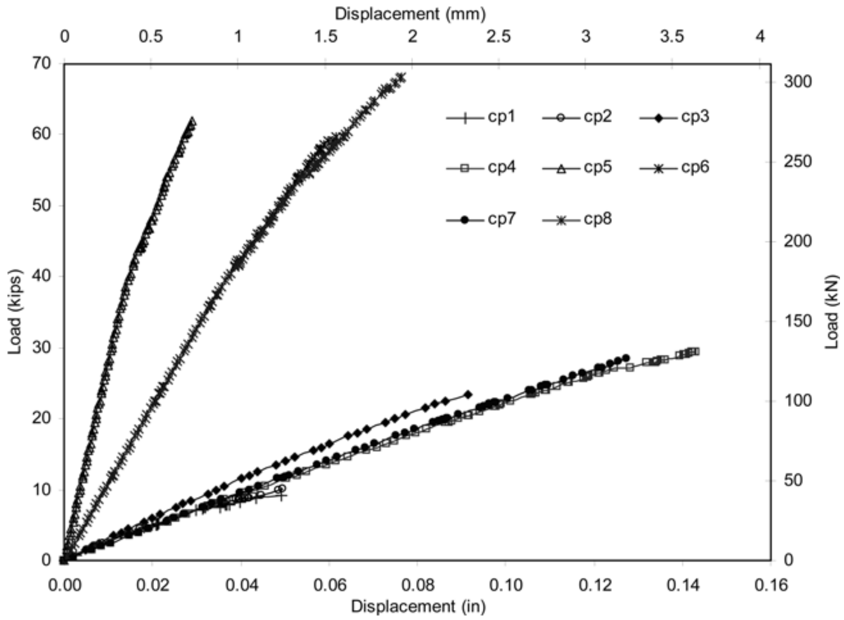

Fig. 6 Load-deformation curves for precast panels

Table 1 Analytical initial tangent stiffness, elastic-limit load and maximum load

Model label	Initial tangent stiffness		Elastic-limit load		Maximum load	
	kN/mm	kips/in	kN	kips	kN	kips
cp1	43	243	20.9	4.7	40.5	9.2
cp2	45	257	20.9	4.7	44.9	10.1
cp3	51	292	46.7	10.5	104.5	23.5
cp4	40	226	82.3	18.5	130.8	29.5
cp5	489	2,792	177.9	40.0	275.3	61.9
cp6	191	1,089	180.1	40.5	266.0	59.8
cp7	41	233	87.2	19.6	126.3	28.4
cp8	191	1,088	180.1	40.5	303.4	68.2

diagonal bars or struts would only be effective if the bars were debonded from the concrete. With the bars bonded to the concrete mass, the bar force would be completely transferred to the concrete mass along the developed length of bar. The developed length for 22 mm diameter (#7) 413.7 MPa (Grade 60) bars and 34.48 MPa (5,000 psi) concrete is only 1.22 m (4 ft), compared to the panel length of 7.32 m (24 ft). In model cp3, by adding reinforcing bars at the loaded regions, the FE model was able to reach higher load prior to termination of the analysis due to a lesser extent of cracking. The elastic-limit load had increased by more than two times though it only improved the initial stiffness marginally by 20%.

Embedding the HSS into the concrete resulted in high stress concentration and early reduction in lateral stiffness as observed in cases cp1 to cp3. The introduction of the HCA in model cp4, to better distribute the anchoring force, significantly increased the elastic-limit load by as much as

76%. A slight reduction (23%) in overall stiffness was not expected since the HSS exhibited higher flexure stiffness than the headed stud anchor. Changing the support condition of the cantilevered bearing supports from pinned (model cp4) to fixed (model cp6) led to the greatest increase (more than five times) in the lateral stiffness. This significant reduction is not unreasonable since the stiffness of a cantilever beam bending in double-curvature is at four times that of a beam bending in simple curvature. Removing the (right) cantilevered bearing support, in model cp5, resulted in a two times increase in stiffness, compared to model cp6. An additional mid-layer of reinforcing bars was added with the intention of confining the concrete around the loaded points. Comparing models cp4 and cp6 with those of cp7 and cp8, respectively, the results indicate no significant reduction in the in-plane stiffness and strength as the result of omitting the center layer. The conventional two layers, one on each face, seems adequate. For model cp8, at 177.9 kN (40 kips), only minor cracks formed in the surface concrete elements adjacent to the loaded HCA. The depth of these cracks was confined to the thickness of the concrete cover and hence would not cause any stiffness or strength degradation. Thus the reinforcement and connection details specified in model cp8 would allow the EDCS (except for the friction damper) to behave elastically as required. It should be pointed out that model cp8 represents only one of the several possible solutions. Further optimization of the EDCS, especially the connection and reinforcement details, is possible but is beyond the scope of the present study.

4. Development of a simplified analytical model

The FEA results supported the EDCS concept as capable of functioning both as a structural brace and an energy absorbing device, the performance of the EDCS as a passive seismic protection system must be evaluated at the building level. Despite the fact that it is possible to model the EDCS and a representative building or structure using FEA techniques discussed earlier, it would be more logical (and efficient) to first reduce the FE model of the EDCS to a simpler mathematical formulation. The strategy adopted here is to represent the in-plane behavior of the EDCS as a two-dimensional assemblage of truss and spring elements as shown in Fig. 7. The (infinitely) rigid truss elements only serve to transmit the axial forces developed in the EDCS to the supporting beam and column. The axial deformations in these elements are made negligible and are oriented as shown to correctly replicate the direction of the forces at the connections. The entire load-deformation characteristic of the EDCS is presented here by a single elastic perfectly-plastic spring element with stiffness K_{EDCS}.

The overall lateral stiffness (K_{EDCS}) of EDCS can be considered as comprising of a series of springs, each capturing the load-deformation of a major component of the system. As shown in Fig. 8, the major components contributing to the lateral stiffness of the assembly are the reinforced concrete panel ($K_{concrete}$), the bearing support ($K_{bearing}$), the headed stud assemblies (K_{stud}), and the damper assembly (K_{damper}). While the stiffnesses of the concrete panel and the (cantilevered) bearing supports may be approximated by theory of elasticity, the load-deformation characteristic of the concrete anchorage (i.e., headed studs and plate) is more complex as it involved the interaction between the embedded studs and concrete matrix. One way to overcome this difficulty is to treat the concrete panel and headed stud assemblies as a single component (K_{panel}) in the stiffness calculation.

The individual springs act together in series based on the load path. The overall lateral stiffness of the EDCS (K_{EDCS}) is related to the individual stiffnesses (k_i) as follows,

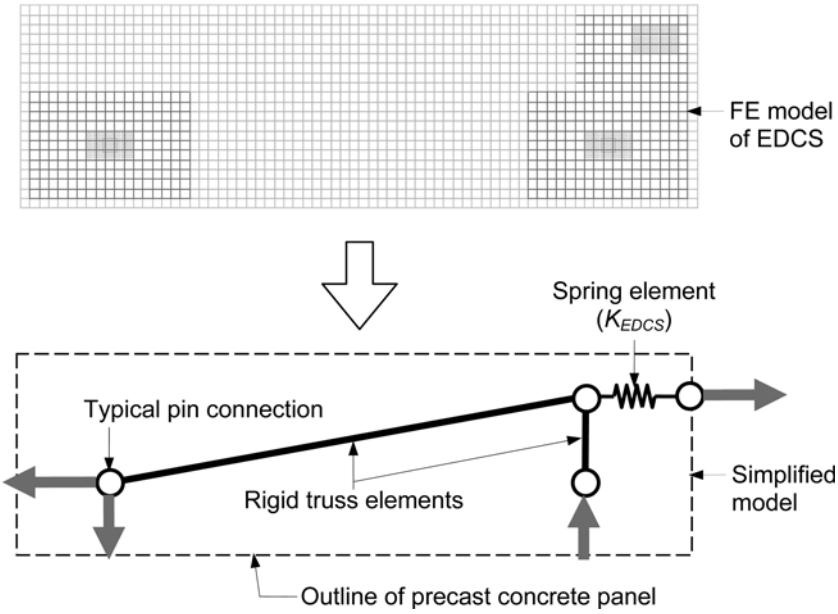

Fig. 7 Simplifying the mathematical model of EDCS

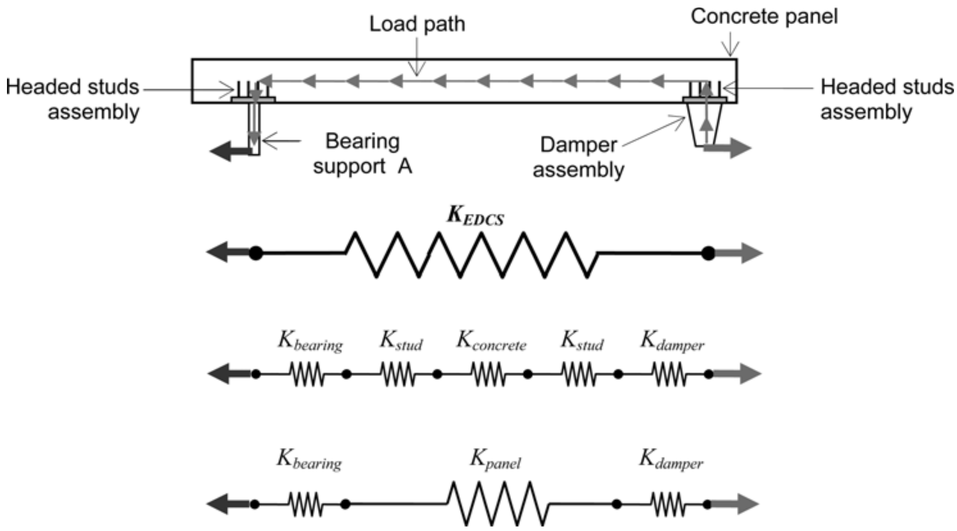

Fig. 8 Components of EDCS stiffness

$$K_{EDCS} = \frac{1}{\sum_{All} \frac{1}{k_i}} \tag{1}$$

The component stiffness coefficients discussed so far are plotted in Fig. 9. Although the ultimate failure load of each major component of the EDCS could be found (from prevailing design codes), it is not necessary to construct the entire load-deformation curve since the lateral load in the EDCS is capped at the design slip load of friction damper as illustrated. All other components are designed

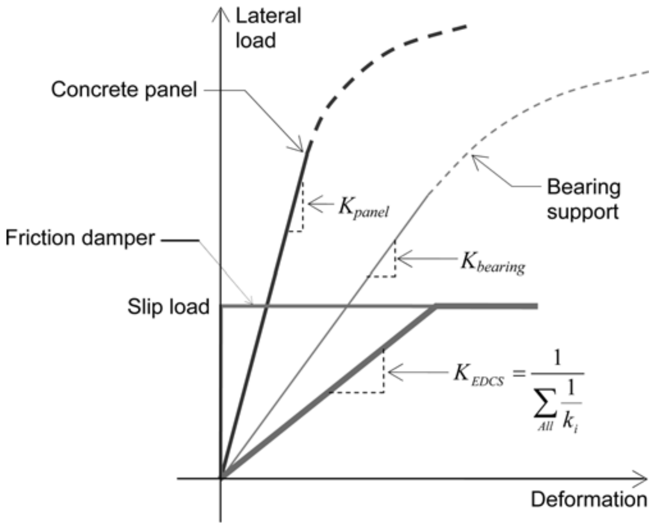

Fig. 9 Load-deformation of EDCS components

to respond elastically throughout the operating range of the damper.

The estimation of the stiffness of the individual component is discussed next. The load-deformation of the friction damper is well documented in literature and hence would not be covered here.

4.1 Estimating concrete panel stiffness

The approach chosen to idealize the concrete panel is to consider it as a cantilevered beam. The overall in-plane response of the concrete panel can be separated into three distinct modes, namely axial, shear and flexure as shown in the Fig. 10. An axial component exists because, for the present study, one of the bearing supports was designed as a roller.

The stiffness coefficients for the three modes of responses can be represented by the following expressions

$$\text{(Axial response)} \qquad K_{C,axial} = \frac{EA_1'}{l'} \tag{2}$$

$$\text{(Shear response)} \qquad K_{C,shear} = \frac{2GA_2'}{3h'} \tag{3}$$

$$\text{(Flexure response)} \qquad K_{C,flexure} = \frac{3EI'}{h'^2} \tag{4}$$

h', l', A_1', A_2' and I' are the "effective" panel height, length, cross-section areas and moment of inertia, respectively. E and G are the modulus of elasticity of reinforced concrete in tension and shear, respectively. The above equations are based on elementary theory of elasticity assumptions of small deflections and plane sections remaining plane after bending (Timoshenko and Goodier 1970). The FEA results revealed that stress distribution (away from the supports) within the panel is approximately linear. Hence it seems appropriate to use the dimensions between the supportsfor the

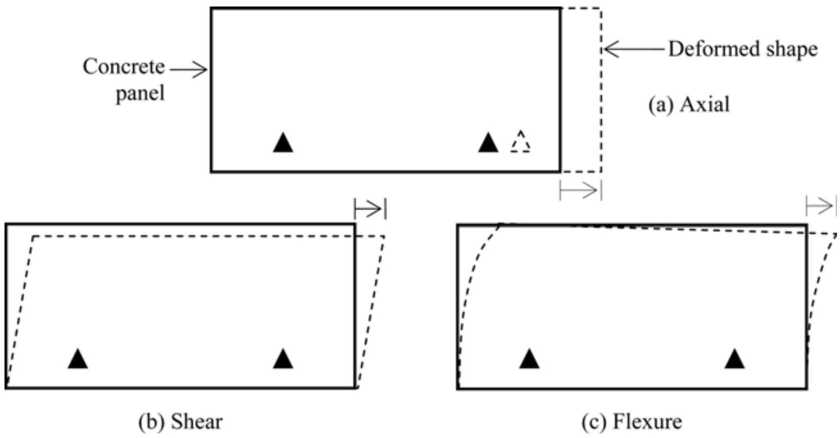

Fig. 10 Response modes for concrete panel

above equations, although it is also not unreasonable to use the overall dimensions of the panels in the above stiffnesses formulation. The overall lateral stiffness of the concrete plane can be determined from the following expression

$$K_{Concreate} = \frac{1}{\dfrac{1}{K_{C,\,axial}} + \dfrac{1}{K_{C,\,shear}} + \dfrac{1}{K_{C,flexure}}} \tag{5}$$

A total of 13 FE models were created in ANSYS to investigate the applicability of the above expressions. Each of these models was similar to model cp5 (with respect to reinforcement layout and connection details) except for the panel dimensions, concrete compressive strength and locations of the HCA's. These parameters were varied so that each model gave a slightly different lateral stiffness value using the equations discussed above. Table 2 summarizes the parameter that was changed for each model. Model pk1 was taken as the control case for this series.

Table 2 FE models of cladding panel

Model	Description
pk1	Identical to cp5; control case. L: 7315.2 mm (288"); H: 2133.6 mm (84"); t: 203.2 mm (8")
pk2	Thickness reduced from 203.2 mm (8") to 154.2 mm (6")
pk3	Thickness increased from 203.2 mm (8") to 254.0 mm (10")
pk4	Height increased from 2133.6 mm (84") to 3352.8 mm (132")
pk5	Length reduced from 7315.2 mm (288") to 4572.0 mm (180")
pk6	Concrete strength reduced from 34.5 MPa (5 ksi) to 27.6 MPa (4 ksi)
pk7	Concrete strength increased from 34.5 MPa (5 ksi) to 41.4 MPa (6 ksi)
pk8	(Bottom) bearing supports moved towards bottom edge by 203.2 mm (8")
pk9	(Bottom) bearing supports moved towards side edges by 304.8 mm (12")
pk10	(Top) loading point moved away from top edge by 203.2 mm (8")
pk11	(Top) loading point moved away from edge by 203.2 mm (8")
pk12	Height increased from 2133.6 mm (84") to 2743.2 mm (108")
pk13	Length reduced from 7315.2 mm (288") to 6096.0 mm (240")

Fig. 11 shows the lateral load-deformation curves. With the exception of model pk6, all curves are linear up to 155.7 kN (35 kips). Model pk6 was specified a low concrete compressive strength which probably led to significant concrete cracking and reduction of stiffness at a significantly lower load.

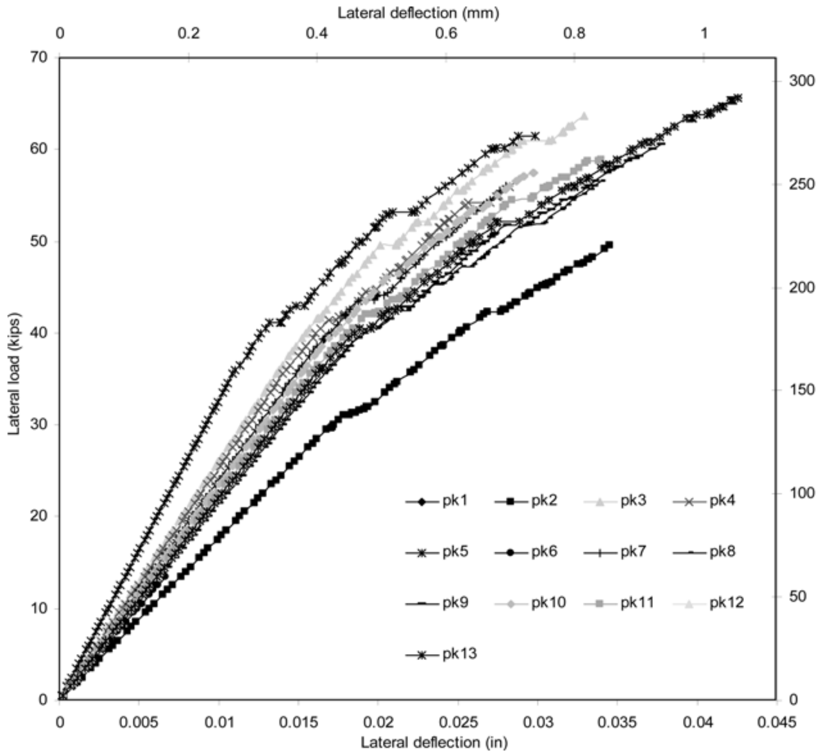

Fig. 11 PK series load-deformation curves

Table 3 Analytical initial tangent stiffness, elastic-limit load and maximum load

Model	Initial tangent stiffness, K_{panel}		Elastic-limit load		Maximum load	
	kN/mm	kips/in	kN	kips	kN	kips
pk1	387	2,212	160.1	36	293.6	66
pk2	309	1,762	133.4	30	222.4	50
pk3	457	2,611	177.9	40	284.7	64
pk4	443	2,530	169.0	38	249.1	56
pk5	572	3,269	160.1	36	271.3	61
pk6	355	2,027	62.3	14	62.3	14
pk7	419	2,395	173.5	39	249.1	56
pk8	380	2,168	160.1	36	253.5	57
pk9	375	2,141	160.1	36	271.3	61
pk10	411	2,347	173.5	39	253.5	57
pk11	394	2,252	155.7	35	262.4	59
pk12	426	2,435	164.6	37	240.2	54
pk13	456	2,604	160.1	36	280.2	63

With the maximum lateral force in the EDCS limited to the 89.0 kN (20 kips) slip load of the friction damper, the EDCS would be expected to remain elastic. In any case, the elastic-limit could be increased by welding additional tail bars to HCA and refining the confinement details. Table 3 summarizes the initial tangent stiffness, maximum load, the elastic-limit load for each model.

By applying regression techniques on the numerical stiffness results, the "effective" dimensions for Eqs. (2)-(5) could be identified. For the axial stiffness, the area (A_1) was taken as the panel gross cross-sectional area. This is reasonable since linear stress distribution was observed to extend from the top edge to the bottom edge of the panel. The horizontal distance between left pin support A and load application point D was used as the "effective" length (l'). For shear response, the shear modulus of elasticity (G) was taken to be 40% of the Young's modulus (ACI 318, 2002). The shear area (A_2) was taken as the entire plan area of the panel. The "effective" height (h') for both shear and flexural response was taken to be the vertical distance between points A and D. With these "effective" dimensions, the following equations were obtained

$$\text{(Axial response)} \quad K_{C,axial} = \frac{EA_1'}{l'} = \frac{E(Ht)}{(L-b_b-b_t)} \tag{6}$$

$$\text{(Shear response)} \quad K_{C,shear} = \frac{2GA_2'}{3h'} = \frac{2(0.4E)[tL]}{3(H-a_b-a_t)} \tag{7}$$

$$\text{(Flexure response)} \quad K_{C,flexure} = \frac{3EI'}{h'^2} = \frac{3E[L^3t/12]}{3(H-a_b-a_t)^3} \tag{8}$$

a_b, a_t, b_b and b_t are the respective edge distances for the headed studs anchors (HCA); E was calculated based on the recommendation by ACI 318 (2002). The overall lateral stiffness of the concrete panel alone (i.e., excluding the deformation of the HCA) was determined from Eq. (5). The calculated stiffness values for each model are summarized in Table 4. The flexural stiffnesses

Table 4 In-plane stiffness of concrete panels

Model	$K_{C,\ axial}$		$K_{C,\ shear}$		$K_{C,\ flexure}$		$K_{Concrete}$		ANSYS Result		Diff. (%)
	$\times10^3$ kN/mm	$\times10^4$ kips/in	$\times10^3$ kN/mm	$\times10^4$ kips/in	$\times10^3$ kN/mm	$\times10^4$ kips/in	$\times10^3$ kN/mm	$\times10^4$ kips/in	$\times10^3$ kN/mm	$\times10^4$ kips/in	
pk1	2.05	1.17	1.62	5.63	5.27	3.01	1.68	0.96	1.66	0.95	-1.5
pk2	1.54	0.88	7.39	4.22	2.98	1.70	1.26	0.72	1.28	0.73	0.8
pk3	2.56	1.46	12.33	7.04	4.96	2.83	2.10	1.20	2.05	1.17	-2.8
pk4	3.20	1.83	4.71	2.69	0.44	0.25	1.82	1.04	1.65	0.94	-10.5
pk5	3.82	2.18	6.16	3.52	0.96	0.55	2.31	1.32	2.45	1.40	6.3
pk6	1.82	1.04	8.81	5.03	3.54	2.02	1.51	0.86	1.49	0.85	-1.1
pk7	2.24	1.28	10.81	6.17	4.34	2.48	1.84	1.05	1.84	1.05	-0.5
pk8	2.05	1.17	8.34	4.76	2.40	1.37	1.63	0.93	1.54	0.88	-6.0
pk9	1.94	1.11	9.86	5.63	3.96	2.26	1.61	0.92	1.63	0.93	0.5
pk10	2.05	1.17	12.05	6.88	7.23	4.13	1.75	1.00	1.77	1.01	1.4
pk11	2.14	1.22	9.86	5.63	3.96	2.26	1.75	1.00	1.72	0.98	-2.3
pk12	2.63	1.50	6.38	3.644	1.07	0.61	1.82	1.04	1.61	0.92	-11.6
pk13	2.57	1.47	8.21	4.69	2.29	1.31	1.94	1.11	2.07	1.18	6.4

are about two orders of magnitude higher than the axial and shear values. It should be pointed out that numerical stiffness values (from ANSYS) in Table 4 did not take into account the deformation of the HCA's while the initial tangent stiffnesses reported in Table 3 (and Table 1) included the HCA's stiffness. The results in Table 4 are plotted in Fig. 12. The approximate beam theory appeared to correlate well with the numerical results. Models pk4 and pk12 gave the highest difference of -10.5% and -11.6%, respectively.

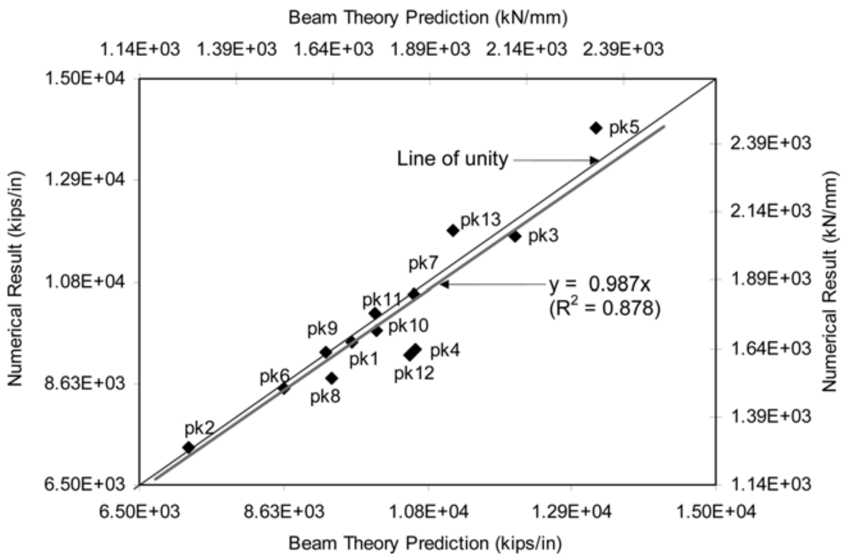

Fig. 12 Comparison of concrete panel stiffness without HCA

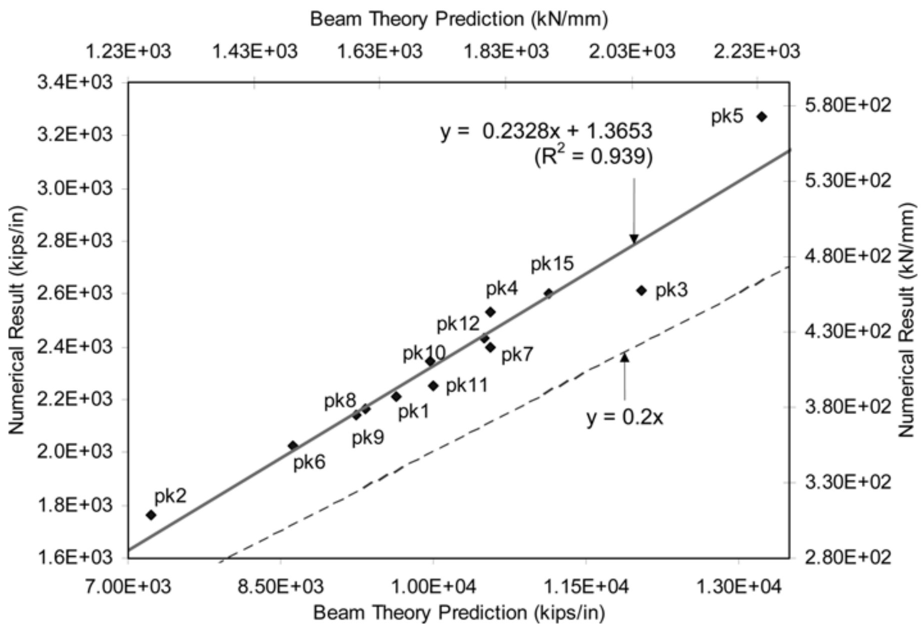

Fig. 13 Comparison of concrete panel stiffness with HCA

Table 5 Applicable range of panel parameters

No.	Parameter	Range
1	Length	2.7 m (108” or 9’) – 7.3 m (288” or 24’)
2	Height	2.1 m (84” or 7’) – 4.0 m (156” or 13’)
3	Thickness	154.2 mm (6”) – 254.0 mm (10”)
4	Concrete Compressive Strength	27.6 MPa (4 ksi) – 41.1 MPa (6 ksi)

Taking into account the flexibility of the HCA, the overall lateral stiffness of the panel was significantly reduced by more than 80%, as shown in Fig. 13. The correlation between the numerical results and beam theory predictions improved slightly as evident from the higher coefficient of determination (i.e., R^2 value). This reduction was not unexpected since the designed HCA was only about one-quarter stiffer than the panel. Due to lack of experimental data and as a conservative estimate, the in-plane stiffness of the panel with HCA was taken to be 20% of that of the concrete panel without HCA (Eq. (9))

$$K_{panel} = 2.0K_{concrete} \tag{9}$$

It should be pointed out that the expressions are applicable for the range of parameters shown in Table 5.

4.2 Estimating bearing support stiffness

The cantilevered bearing supports for conventional architectural precast cladding system are typically not designed for lateral load; friction force developed between the cantilevered section and shim is assumed to be sufficient to resist any unanticipated lateral load. For the EDCS, the bearing support A, must be specifically designed for the slip load of the friction damper. The stiffness of the bearing support is a function of the relative out-of-plane flexibility of the bearing support and the concrete panel (Fig. 14).

If the panel is infinitely stiff with respect to the bearing support, the following equations for the out-of-plane stiffness would apply:

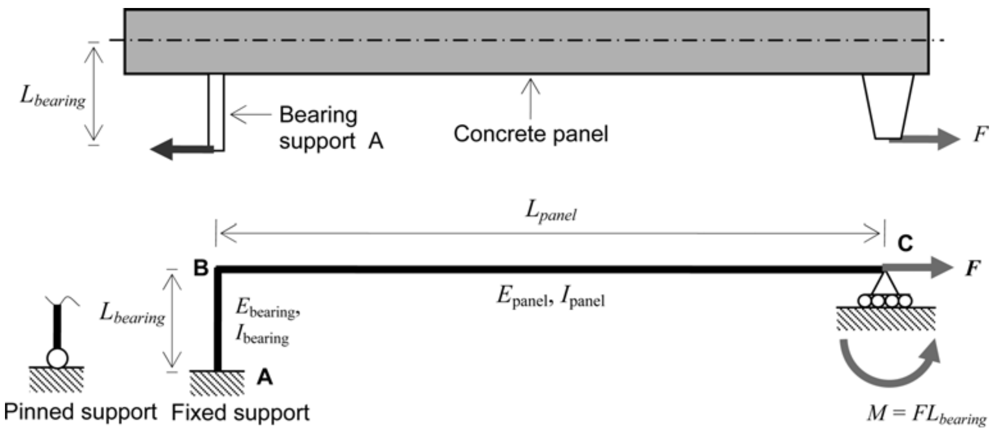

Fig. 14 Simplified model for out-of-plane response

$$\text{(Pinned support)} \quad K_{bearing} = \frac{3(EI)_{bearing}}{L^3_{bearing}} \tag{10}$$

$$\text{(Fixed support)} \quad K_{bearing} = \frac{12(EI)_{bearing}}{L^3_{bearing}} \tag{11}$$

$E_{bearing}$ and $I_{bearing}$ are the Young modulus of elasticity and moment of inertia of the bearing support, respectively; $L_{bearing}$ is the "effective" cantilevered length. If, however the concrete panel is considerably more flexible than the bearing support, the above equations would grossly overestimate the bearing support stiffness. Taking into account the out-of-plane flexibility of the concrete panel, it can be shown (from classical geometrical or energy methods) that the lateral stiffnesses of the panels with the bearing supports are represented by the following

$$k_{F,pinned} = \frac{3(EI)_{bearing}}{L^3_{bearing}}\left[\frac{2}{2+3\alpha}\right] \tag{12}$$

(Pinned support)

$$k_{fixed} = \frac{12(EI)_{bearing}}{L^3_{bearing}}\left(\frac{\alpha+3}{7\alpha+3}\right) \tag{13}$$

(Fixed support)

$$\text{Where} \quad \alpha = \frac{\left(\frac{EI}{L}\right)_{bearing}}{\left(\frac{EI}{L}\right)_{panel}} \tag{14}$$

The stiffness coefficient values calculated using Eqs. (12) and (13) were compared to the numerical results from FE model cp7 (pinned support condition) and model cp8 (fixed support) in Table 6. In deriving the closed-form equations, the bearing-panel joint was assumed to be infinitely

Table 6 Bearing stiffness for different support conditions

Source	Bearing length $L_{bearing}$		Bearing stiffness			
			Pinned		Fixed	
	(mm)	(in)	(kN/mm)	(kips/in)	(kN/mm)	(kips/in)
ANSYS (cp7)			55	312		
ANSYS (cp8)					453	2,589
Closed-formed solution			Eq. (12)		Eq. (13)	
	330	13	93	529	418	2,387
	356	14	78	447	346	1,974
	406	16	57	328	246	1,403

Definition of bearing length
Headed studs Concrete panel

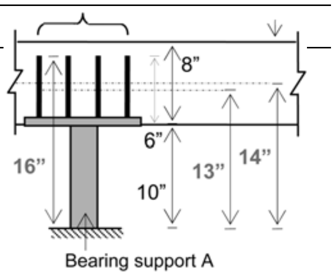

Notes:
$E_{bearing} = 2 \times 10^5$ MPa (29×10^6 psi), $E_{panel} = 2.8 \times 10^4$ MPa (4×10^6 psi), $I_{bearing} = 2.0 \times 10^7$ mm^4 (48.3 in^4), $I_{panel} = 5.87 \times 10^8$ mm^4 (3,584 in^4), $L_{panel} = 5.88$ m (232 in.)

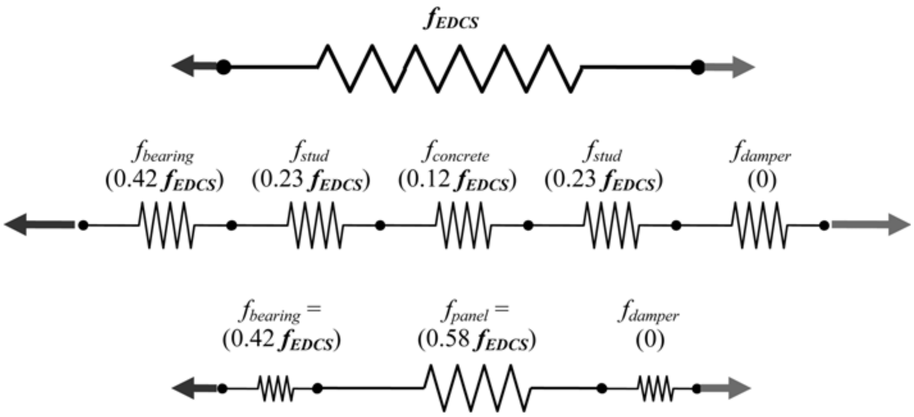

Fig. 15 Flexibility coefficients of EDCS components

rigid. Because the HCA exhibited some degree of rotational flexibility, the "effective" bearing length would vary with different support conditions. Three "effective" cantilevered lengths of the bearing support were investigated here as shown in Table 6. The shortest length of 330 mm (13 in.) was the distance between the bearing end supports to the center of the stud groups. The distance from the tip of the studs to the fixed end support was 406 mm (16 in.) while the distance to the center of the panel was 356 mm (14 in.).

Under both pinned and fixed support conditions, increasing the bearing length has the same effect of reducing the stiffness of the bearing support. Comparing the closed-form solutions (i.e., Eqs. (12) and (13)) with the numerical results, it appears that the distance to the center of the stud groups should be used for fixed support condition whereas for pinned condition, the distance to the tip of the studs; giving conservative estimates of the bearing stiffness. A pinned support led to an appreciable reduction of stiffness at relatively low load level due to significant cracking around the concrete anchors. Hence, to achieve a high out-of-plane fixity in the field, a combination of pinned bearing support with welded shear plates could be used.

To facilitate the FEA of architectural cladding panels, the panels are often modeled as uncracked and rigid (Petkovski and Waldron 1995, Goodno and Craig 1998). The present study has shown that this may not be the case as the overall lateral stiffness of the panel is sensitive to the stiffness of its contributing components. Fig. 15 summarizes the estimated contribution of each component in the EDCS in terms of flexibility coefficients (i.e., reciprocal of the stiffness); f_{EDCS}, $f_{bearing}$, f_{stud}, $f_{concrete}$ and f_{panel} are the flexibility coefficients of the EDCS, (fixed) cantilevered bearing support, headed stud assembly, concrete panel and the panel with HCA, respectively. The results show that the assumption of an infinitely stiff precast concrete panel would not be appropriate here.

5. Conclusions

The present study has developed an innovative design concept that integrates both architectural and structural performance into the EDCS. The EDCS is intended to give the designer an alternative method of improving the earthquake resistance of a building. In the present research, extensive analytical studies were performed to validate the design and performance of the EDCS. Based on the assumptions made in design, modeling, and analyses presented in this study, the following summary and conclusions can be stated:

1. From the literature reviews it is concluded that extensive cladding damage, which constitutes a significant part of the cost of nonstructural damage, has been frequently observed in past earthquakes. Modern earthquake-resistant design attempts to reduce such earthquake-induced damage through connection details aim at isolating the cladding panels from the supporting structure, thereby minimizing the damaging interaction effects.
2. It is not always necessary to minimize the cladding-structure interaction to prevent damage to the precast concrete cladding. Past research has married the cladding-structure interaction with the energy dissipation concept. However, these studies have been focused primarily on energy dissipation and are limited to floor-to-floor high cladding panels. From the literature reviews and evidence of significant research support on floor-to-floor high energy dissipating panels, it is concluded that the industry would be interested in developments in spandrel type energy dissipating cladding panels.
3. The EDCS developed in the present study introduces an alternative system that can provide significant lateral stiffness and energy dissipation to the building, with the primary objective of reducing the building response to earthquake ground motions. The EDCS was developed as a spandrel type cladding panel since modern building facades typically require continuous strip openings for window installations or ventilation requirements.
4. Despite the lower lateral stiffness of the individual partial height spandrel bracing (as compared to full-height cross-bracing), it is concluded that the perimeter spandrel bracing system can provide lateral stiffness that can be relied upon as a form of bracing system. Because the spandrel bracings are distributed over the building perimeter, they are effective in distributing the column axial forces and reducing torsional effects.
5. In this study, a friction damper system was employed that is drift-sensitive and will achieve the required slip load at low drifts.
6. Because the design of the EDCS is very similar to that of conventional architectural precast concrete cladding system, the preliminary design of the EDCS components could be based on existing design guidelines on the conventional cladding system. The FEA was then employed to check and further refine the design.
7. The present study also suggested that a commercially available finite element analysis package, ANSYS (Version 9), is capable of modeling the complex nonlinear behavior of structural concrete through the availability of a concrete element (i.e., SOLID65). The simple finite element modeling strategy adopted for both reinforced concrete, headed stud anchors and panel connections were found to be adequate.
8. FEA results showed that diagonal bars or brace placed between the support and the load application would only be effective if the bars were debonded from the concrete. With the bars bonded to the concrete mass, the bar force would be completely transferred to the concrete mass along the developed length of bar due to the length of the spandrel panel. The nonlinear FEA results showed that precast concrete panels can be designed to remain essentially elastic up to the slip load of the friction damper if adequate reinforcement and proper detailing of the connections are provided.
9. The results from the FEA also showed that embedding the HSS into the concrete resulted in high stress concentration and early reduction in lateral stiffness. The HCA would provide better distribution of anchoring force than embedded HSS section, significantly increased the

elastic-limit load by as much as 76%.

10. Changing the support condition of the cantilevered bearing supports from pinned to fixed led to as much as five times increase in the lateral stiffness of the panel.
11. The FEA results showed that the additional center layer of reinforcing bars was not necessary because the FEA results indicate no significant reduction in the in-plane stiffness and strength as a result of omitting the center layer. Therefore, it is concluded that the conventional two curtains of reinforcement, one on each face, is adequate.
12. The in-plane response of the concrete panel could be approximated by three distinct modes: axial, shear and flexure. Closed-form expressions quantifying the contribution of each mode were developed based on the FEA results. From the study it can be concluded that, within the range of applicability, the approximate elastic beam solutions were adequate for the developed EDCS and would be useful for preliminary design purposes.
13. By taking into account the flexibility of the HCA, the FEA results revealed that the overall lateral stiffness of the panel could be significantly reduced by more than 80%. Therefore, the stiffness in addition to the strength of the concrete anchorage system must be considered in the design for the EDCS.
14. The FEA results revealed that the precast concrete panel with HCA can contribute as much as 58% to the overall lateral flexibility of the EDCS unit. It is therefore concluded that the (common) assumption of an infinitely stiff precast concrete panel may not be appropriate.

The analytical stiffness and strength characteristics of the proposed EDCS have been investigated in the present paper through combination of FEA technique and classical structural analysis method. The result is a simplified mathematical model that can be incorporated into suitable building models to evaluate its performance. The proposed EDCS has a dual purpose of being part of the building envelope and as part of the LFRS. Besides the structural design viewpoint, considerations pertaining to the architectural and constructional aspects are also important for consideration as design refinements will be made in follow-up studies.

References

American Concrete Institute (ACI) Committee 318. (2002), *Building Code Requirements for Structural Concrete (ACI 318-02) and Commentary (ACI 318R-02)*, ACI, Farmington Hills, Michigan.

Arnold, C., Hopkins, D.C. and Elsesser, E. (1987), *Design and Detailing of Architectural Elements for Seismic Damage Control*, Building Systems Development, Inc., KRTA Limited and Forell/ Elsesser Engineers, San Mateo, CA.

Craig, J.I., Goodno, B.J., Pinelli, J.P. and Moor, C. (1992), "Modeling and evaluation of ductile cladding connection systems for seismic response attenuation in buildings", *Proceedings, 10th World Conference on Earthquake Engineering*, Rotterdam, Netherlands, 4183-4188.

Ellis, B.R. (1980), "An assessment of the accuracy of predicting the fundamental natural frequencies of buildings and the implications concerning the dynamic analysis of the structures", *Proceedings, Institution of Civil Engineers, Part II*, **69**, 763-776.

El-Gazairly, L.F. and Goodno, B.J. (1989), "Dynamic analysis of a high-rise building damaged in the mexico earthquake including cladding-structure interaction", *Proceedings, International Symposium on Architectural Precast Concrete Cladding – Its Contribution to Lateral Resistance of Buildings*, PCI, Chicago, IL, 257-286.

Fanning, P. (2001), "Nonlinear models of reinforced and post-tensioned concrete beams", *Elect. J. Struct. Eng.*, **2**, 111-119.

Gaiotti, R. and Smith, B.S. (1992), "Stiffening of moment-resisting frame by precast concrete cladding", *PCI J.*, **37**(5), 80-92.

Goodno, B.J. and Craig, J.I. (1998), "Ductile cladding connection systems for seismic design", *Report No. NIST GCR 98-758*, National Institute of Standards and Technology, Gaithersburg, MD.

Goodno, B.J., Craig, J.I., El-Gazairly, L.F. and Hsu, C.C. (1992), "Use of advanced cladding systems for passive control of building response in earthquakes", *Proceedings, 10th World Conference on Earthquake Engineering*, Madrid, Spain, 4195-4200.

Goodno, B.J. and Will, K.M. (1978), "Dynamic analysis of a high-rise building including cladding-structure interaction effects", *Proceedings, Conference on Computers in Civil Engineering*, Atlanta, GA, 623-638.

Grigorian, C.E., Yang, T.S. and Popov, E.P. (1993), "Slotted bolted connection energy dissipators", *Earthq. Spect.*, EERI, **9**(3), 491-504.

Idelsohn, S.R., Onate, E. and Dvorkin, E.N., eds. (1998), *Computational Mechanics. New Trends and Applications*, CIMNE, Barcelona, Spain.

Maneetes, H. (2007), "Development of a seismic dissipating mechanism for precast concrete cladding panels", Ph.D. Thesis, Pennsylvania State University, University Park, PA.

McMullin (2000), http://www.engr.sjsu.edu/mcmullin/research/cladding/.

Meyyappa, M., Palsson, H. and Craig, J.I. (1981), "Modal parameter estimation for a highrise building using ambient response data taken during construction", *Proceedings, 2nd Specialty Conference on Dynamic Response of Structures: Experimentation, Observation, Prediction, and Control*, Atlanta, GA, 141-151.

Pall, A.S., Marsh, C. and Fazio, P. (1980), "Friction joints for seismic control of large panel structures", *Journal of Prestressed Concrete Institute*, **25**(6), 38-61.

Petkovski, M. and Waldron, P. (1995), "Seismic behavior of reinforced concrete frames with energy dissipating cladding", *European Seismic Design Practice*, Balkema, Rotterdam, Netherlands.

Pinelli, J.P., C., Craig, J.I., Goodno, B.J. and Hsu, C.C. (1993), "Passive control of building response using energy dissipating cladding connections", *Earthq. Spect.*, **9**(3), 529-546.

Precast/Prestressed Concrete Institute (PCI). (1989), *Architectural Precast Concrete*, 2nd ed., PCI, Chicago, IL.

Precast/Prestressed Concrete Institute (PCI). (2004), *PCI Design Handbook: Precast and Prestressed Concrete*, 6th ed., PCI, Chicago, IL.

Timoshenko, S.P. and Goodier, J.N. (1970), *Theory of Elasticity*, 3rd ed., McGraw-Hill, Singapore.

Uchida, N., Aoygai, T., Kawamura, M. and Nakagawa, K. (1973), "Vibration test of steel frame having precast concrete panels", *Proceedings, 5th World Conference on Earthquake Engineering*, Rome, Italy, 1167-1176.

Wiss, J.F and Curth, O.E. (1970), "Wind deflections of tall concrete frame buildings", *J. Struct. Div.*, ASCE, **96**(ST7), 1461-1480.

Wolanski, A.J. (2004), "Flexural behavior of reinforced and prestressed concrete beams using finite element analysis", *Master Thesis*, Marquette University, Milwaukee, WI.